Available online at BCREC website: https://bcrec.id

Bulletin of Chemical Reaction Engineering & Catalysis, 15 (3) 2020, 674-686

Research Article

Studies on Epoxidation of Tung oil with Hydrogen Peroxide Catalyzed by Sulfuric Acid

Eni Budiyati[1,2*], Rochmadi Rochmadi[1], Arief Budiman[1], Budhijanto Budhijanto[1]

[1]Department of Chemical Engineering, Faculty of Engineering, Universitas Gadjah Mada, Jl. Grafika 2, Yogyakarta, Indonesia
[2]Department of Chemical Engineering, Faculty of Engineering, Universitas Muhammadiyah Surakarta, Jl. A. Yani, Pabelan, Kartasura, Surakarta 57102, Indonesia

Received: 22nd June 2020; Revised: 11st August 2020; Accepted: 13rd August 2020; Available online: 14th August 2020; Published regularly: December 2020

Abstract

Tung oil with an iodine value (IV) of 99.63 g I_2/100 g was epoxidized in-situ with glacial acetic acid and hydrogen peroxide (H_2O_2), in the presence sulfuric acid as catalyst. The objective of this research was to evaluate the effect of mole ratio of H_2O_2 to unsaturated fatty acids (UFA), reaction time and catalyst concentration in Tung oil epoxidation. The reaction kinetics were also studied. Epoxidation was carried out for 4 h. The reaction rates and side reactions were evaluated based on the IV and the conversion of the epoxidized Tung oil to oxirane. Catalytic reactions resulted in higher reaction rate than did non-catalytic reactions. Increasing the catalyst concentration resulted in a large decrease in the IV and an increase in the conversion to oxirane at the initial reaction stage. However, higher catalyst concentration in the epoxidation reaction caused to a decrease in reaction selectivity. The mole ratio of H_2O_2 to UFA had an influence identical to the catalyst concentration. The recommended optimum mole ratio and catalyst concentration in this study were 1.6 and 1.5%, respectively. The highest conversion was 48.94% for a mole ratio of 1.6. The proposed kinetic model provided good results and was suitable for all variations in reaction temperature. The activation energy (E_a) values were around 5.7663 to 76.2442 kcal/mol.

Keywords: Tung Oil; In-situ Epoxidation; Heterogeneous Kinetics Model; Sulfuric Acid; Hydrogen Peroxide

How to Cite: Budiyati, E., Rochmadi, R., Budiman, A., Budhijanto, B. (2020). Studies on Epoxidation of Tung oil with Hydrogen Peroxide Catalyzed by Sulfuric Acid. *Bulletin of Chemical Reaction Engineering & Catalysis*, 15(3), 674-686 (doi:10.9767/bcrec.15.3.8243.674-686)

Permalink/DOI: https://doi.org/10.9767/bcrec.15.3.8243.674-686

1. Introduction

Many efforts have been made to substitute petroleum with renewable eco-friendly natural resources. Vegetable oils can be a suitable alternative in this regard because of their abundant availability. In industry, vegetable oils are converted into epoxidized vegetable oils (EVOs). EVOs are intermediate compounds that possess highly reactive oxirane rings and can be utilized in the manufacture of soaps, epoxy resins, polyol, and food products. Specifically, epoxidized fatty acid derivatives from vegetable oils can be used as additives in lubricants, as stabilizers and plasticizers for polymers or polyesters, and in the manufacture of plastics and polyurethane. The commercialization of EVOs has been

* Corresponding Author.
E-mail: eb112@ums.ac.id (E. Budiyati)

undertaken on a large scale, e.g. epoxidized soybean oil (ESO) and epoxidized linseed oil (ELO) [1,2].

Although ESO and ELO have been produced commercially and have many advantages, they have sparked a debate over their sustainability. The use of edible-based renewable feedstuffs, such as soy and linseeds, triggered an argument about "feedstuff versus continuity" [3]. As a result of this debate, it became advisable to use non-edible-based renewable feedstuffs to maintain its continuity and does not interfere the food needs. Some research has been pursued to embody "truer sustainability (continuity)" through the synthesis of epoxidized vegetable oils from non-edible feedstocks such as rubber seed oil [4,5], castor oil [6,7], mahua oil [8], and Karanja oil [9]. Similar research has been conducted on jatropha oil [10], cottonseed oil [11], nahor [12], canola oil [13], camelina oil [14], giraneol oil [15], and perrila oil [16].

Tung plant (*Reutealis trisperma* (Blanco) Airy Shaw) is found in Southeast Asia. This plant can flower and produce fruit once a year, at the end of the rainy season, and it can grow in lowlands and in moderate plains. Tung seed kernel can produce crude oil of 45%-50% yield with a high content of unsaturated fatty acids (UFA). The UFAs in Tung oil are produced from the extraction, degumming, and hydrolysis of Tung seed. The oil contains several UFAs, among other oleic acids, linoleic acids, and α-oleo stearate acids. The α-oleo stearic acids are high quality UFAs that can be converted to epoxides, but they are toxic [17]. For this reason, Tung oil is categorized as a non-edible oil. Therefore, Tung oil is a qualified vegetable oil that can be reacted with peroxyacetic acid, produced in-situ, to generate EVOs because it is non-edible and its chemical structure includes a double bond.

A great deal of research on Tung oil has been performed. Tung seed oil was used in the synthesis of methyl ester [18]. It was transformed into oleo stearic acid diethanol amide (EADEA) for preparation in biobased polyurethane by methyl-esterification [19], as pressure-sensitive stickies from Tung oil by Diels-Alder method [20]. Tung-acid-maleic triacrylate and Tung-maleic tetra acrylate were two types of UV-curable active monomers synthesized from Tung oil [21]. None of these studies addressed Tung oil epoxidation.

Studies on Tung oil epoxidation have been previously conducted [22,23]. In a past study, epoxidized dicarboxylic acid dimethyl ester can be synthesized from Tung oil. It used as a supplementary thermal stabilizer of PVC and as a plasticizer [22]. Phosphoric acid was used as a catalyst in its epoxidation and formic acid as an active oxygen carrier. This study did not address the effect of process variables and the kinetics of Tung oil epoxidation. The in-situ epoxidation of EVOs from Tung oil using peroxyacetic acid has been previously carried out [23]. This study evaluated the influence of temperature on the epoxidation of Tung oil and the kinetics of homogeneous reactions without considering side reactions. In this study, increasing temperature caused an increase in both the oxirane number of EVOs and the reaction rate constant. The reported results indicate that the homogeneous kinetic model is not suitable for high temperatures (60 °C and above).

Despite these studies, a heterogeneous kinetics model and the influence of other reaction variables have not yet been evaluated. In addition, heterogeneous kinetics studies of some vegetable oils have been widely conducted; however, there is a lack of information on Tung oil as raw material. Several studies on the kinetics of epoxidation of vegetable oils, such as soybean [24-29], canola oil [30,31], grape seed oil [32], cotton seed oil [11], karanja oil [9], mahua oil [8], jatropha oil [33], MEPOL oil [34], castor oil [35], and parkia biglobosa seed oil [36] have been carried out.

This paper aims to investigate the effects of catalyst concentration and the mole ratio of H_2O_2 to UFA on the IV, conversion to oxirane, and selectivity of the epoxidation reaction. This study also evaluates the heterogeneous kinetic model of a side reaction in Tung oil epoxidation. This kinetic model is expected to reveal the reason for the incompatibility of the use of homogeneous reaction kinetics at higher temperatures.

2. Materials and Methods

2.1 Materials

Tung seeds (*Reutealis trisperma* (Blanco) Airy Shaw) containing 66.17% oleo stearic acid, 21.72% palmitic acid, 0.27 % linoleic acid, 9.58% oleic acid, and 2.26% other saturated fatty acids were supplied directly by the farmers from the Sulawesi and Majalengka areas of Indonesia. Then, the seeds were extracted, degummed, hydrolyzed, and purified to obtain the fatty acids of Tung oil (as raw material for reactions). Glacial acetic acid (AR Grade), hydrobromic acid in acetic acid (47 wt%), aqueous hydrogen peroxide (30 wt%), sodium thiosul-

fate, Wijs solution, and potassium iodide were purchased from CV. Multikimia, Yogyakarta, Indonesia. Sulfuric acid 98 wt%, crystal violet indicator, and potassium hydrogen phthalate were purchased from CV. General Labora, Yogyakarta, Indonesia.

2.2. Experimental Apparatus

The epoxidation processes were conducted in a glass three-neck flask reactor with a 250 mL capacity equipped with a magnetic stirrer 2 cm inside diameter, thermometer, and a reflux condenser. The speed of stirring was maintained at 500 rpm (with an accuracy of ±5 rpm). The reactor assembly was submerged in the water bath to maintain the reaction temperature (with an accuracy of ± 0.2°C).

2.3. Epoxidation Process

Tung oil (70 grams) and the required amount of glacial acetic acid were charged into the reactor. The mole ratio of Tung oil to glacial acetic acid was 2:1. Certain volume of sulfuric acid catalyst was added then into the reactor. The mixture was stirred at a constant speed and heated to the desired reaction temperature. Once the desired temperature was reached, a certain volume of aqueous hydrogen peroxide (H_2O_2) was appended dropwise into the reactor over 30 min. The reaction was carried out for 4 h. The initial time (t = 0) was set upon completion of the addition of H_2O_2 into the reactor. Samples were removed during the reaction at 30, 60, 90, 120, 150, 180, 210, and 240 min. These samples were cooled to ambient temperature, and were separated between the epoxidized Tung oil (organic or oil phase) and the aqueous phase by a separating funnel. The oil phase was washed with warm distilled water and centrifuged to purify the epoxide from the impurities. The samples were analyzed the iodine value and oxirane number.

The number of moles of hydrogen peroxide were 1.2, 1.4, 1.6, and 1.8 times that of the fatty acid. These variations referenced previous studies with other types of vegetable oils [8,11,12,30]. They showed that the optimum conditions for the epoxidation reaction were obtained in a certain range. Concentrations of the catalysts in the reaction were 0, 1.5, 3, and 4.5% (wt.), which was in accordance with previous research [8,11]. These percentages were determined based on the total weight of glacial acetic acid and aqueous hydrogen peroxide. The reaction temperatures used in data retrieval to evaluate the reaction kinetics model were 40, 50, 60, and 70°C.

2.4. Analysis

The iodine value was determined using the Wijs solution, which reacts with double bonds in UFAs. Historically, iodine has been detected using natrium thiosulfate ($Na_2S_2O_3$). Iodine values were determined using the Wijs method [37], and calculated with Eq. (1),

$$IV = \frac{(B-A)\times N_{thio}\times 12.69}{m} \quad (1)$$

where IV is the iodine value of the sample (unsaturated fatty acids and epoxidized Tung oil), B and A are the volume of natrium thiosulfate needed for titration of blank solution and sample (mL), respectively. N is the natrium thiosulfate solution normality (N), and m is the mass of sample (g).

The oxirane number or oxirane oxygen content was analyzed using a hydrobromic acid solution in glacial acetic acid [37], and calculated with Eq. (2),

$$Oxirane\,oxygen\ content = \frac{V\times N\times 1.6}{m} \quad (2)$$

where V is volume of titration (mL), N is the hydrogen bromide normality (N), and m is the mass of the sample (g).

From the oxirane number, the relative conversion of double bonds to oxirane can be determined with Eq. (3) [11],

$$Conversion\,to\,oxirane = \frac{OO_{ex}}{OO_{theoritical}}\times 100\% \quad (3)$$

where OO_{ex} refers to the experimentally calculated content of oxirane oxygen, and $OO_{theoritical}$ refers to the theoretical maximum oxirane oxygen content in 100 grams of Tung oil, calculated using Equation [11],

$$OO_{theoritical} = \left\{\frac{IV_0/2A_i}{\left[100+(IV_0/2A_i)A_0\right]}\right\}A_0\times 100 \quad (4)$$

where A_0 (16 g/mol) and A_i (127 g/mol) are relative atomic weights of oxygen and iodine, respectively, and IV_0 is the initial iodine value of Tung oil (99.632 g/100 g oil).

The selectivity can be determined with the Equation (5).

$$Selectivity = \frac{OO_{ex}}{OO_{resulted}}\times 100\% \quad (5)$$

where $OO_{resulted}$ is the theoretically resulted oxirane number that is equivalent to the reacted mole number of double bonds in UFA and can be calculated using equation (6), where IV_i represents the iodine values of epoxidized Tung oil (sample).

$$OO_{resulted} = \left\{ \frac{\left(IV_0 - IV_i\right)/2A_i}{\left[100 + \left(\left(IV_0 - IV_i\right)/2A_i\right)A_0\right]} \right\} A_0 \times 100 \quad (6)$$

2.5. The Heterogeneous Kinetics Model

In this kinetics model, the method to produce the epoxidized Tung oil involved several processes, namely the process of peroxyacetic acid (PAA) formation, equilibrium phase (between the aqueous phase and the organic (oil) phase) formation, as well as an epoxidation reaction. In addition, because of the highly reactive nature of the epoxide compound, it is likely that there were side reactions.

PAA can be used to break down the double bonds of UFA. It was formed by reacting hydrogen peroxide and glacial acetic acid generated in-situ. The reaction was reversible and occurred in the aqueous phase. Thus, there will be an equilibrium between the mixture of reactants and products. The presence of strong acid catalysts (H_2SO_4) in this reaction can accelerate the occurrence of equilibrium. The formation of PAA can be described according to equations (7) to (9).

The first step was the protonation of the carbonyl oxygen from acetic acid, which produced an intermediate compound 1 (IC1). The second step was regarded as the rate determining step. This step controlled the overall reaction rate of the formation of PAA. The third reaction occurred rapidly (k_2>>>k_3) because the second step involved more complex processes (i.e. breaking and forming of bonds) when compared to the third step (only bond formation).

$$\frac{d\left[IC1\right]_{aq}}{dt} = k_1\left[AA\right]_{aq}\left[H^+\right]_{aq} - k_{-1}\left[IC1\right]_{aq} - k_2\left[IC1\right]_{aq}\left[PA\right]_{aq} \quad (10)$$

Assuming the process is pseudo state, the concentration of IC1 is obtained as shown in the following equation:

$$\left[IC1\right]_{aq} = \frac{k_1\left[AA\right]_{aq}\left[H^+\right]_{aq}}{k_{-1} + k_2\left[PA\right]_{aq}} \quad (11)$$

Before epoxidation occurred, the PAA was transferred from the aqueous phase to the oil or organic phase. Rapid stirring served to decrease the thickness of the film between phases, such that the mass transfer rate was much faster than the chemical reaction rate. In this case, the mass transfer process can be stated in the form of an equilibrium. Some compounds that remain in the reactions include acetic acid (AA), water (H_2O), catalysts (H^+), and hydrogen peroxide (PA), also present in the phase equilibrium.

$$PAA_{aq} \rightleftharpoons PAA_{org} \quad (12)$$

$$AA_{aq} \rightleftharpoons AA_{org} \quad (13)$$

$$H_2O_{aq} \rightleftharpoons H_2O_{org} \quad (14)$$

$$H^+_{aq} \rightleftharpoons H^+_{org} \quad (15)$$

The correlation between concentration in the aqueous phase and organic phase is shown in the following equations (16), where K_i value is the equilibrium constant of each component (PAA, AA, H_2O, and H^+).

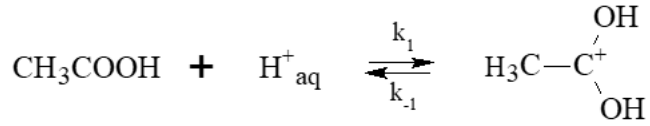

(7)

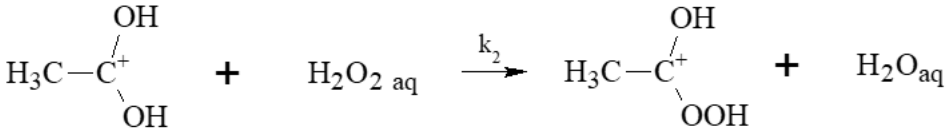

(8)

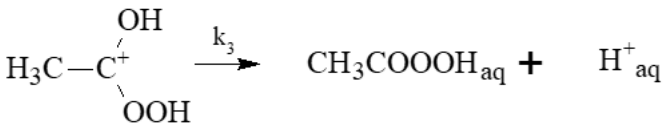

(9)

$$[PAA]_{org} = \frac{[PAA]_{aq}}{K_{PAA}} \quad (16)$$

$$[AA]_{org} = \frac{[AA]_{aq}}{K_{AA}} \quad (17)$$

$$[H_2O]_{org} = \frac{[H_2O]_{aq}}{K_{H_2O}} \quad (18)$$

$$[H^+]_{org} = \frac{[H^+]_{aq}}{K_{H^+}} \quad (19)$$

The epoxidation reaction between the double bond or UFA in Tung oils and PAA that produced epoxidized Tung oil (EP) occurred in the organic phase.

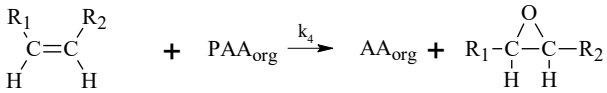

(20)

Protonation of epoxidized Tung oil by H^+_{org}:

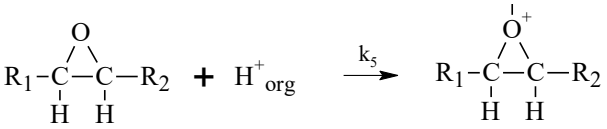

(21)

Reactions of protonated epoxide with AA and H_2O in the organic phase:

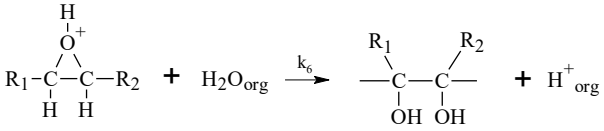

(22)

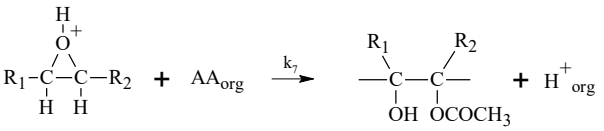

(23)

From the above reaction equations, the concentrations of several components are derived from the mass balance. The obtained results can be written as follows (Equations (24)-(34)).

with,

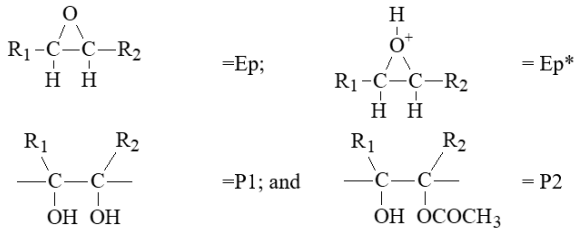

Eq. (11) and Eq. (24) – Eq. (33) are the simultaneous ordinary differential equations (ODE),

$$\frac{d[H^+]_{aq}}{dt} = -k_1[AA]_{aq}[H^+]_{aq} + k_{-1}[IC1]_{aq} + k_2[IC1]_{aq}[PA]_{aq} - k_5'[H^+]_{aq}[Ep]_{org} + k_6'[AA]_{aq}[Ep^*]_{org} + k_7'[H_2O]_{aq}[Ep^*]_{org} \quad (24)$$

$$\frac{d[AA]_{aq}}{dt} = -k_1[AA]_{aq}[H^+]_{aq} + k_{-1}[IC1]_{aq} + k_4'[PAA]_{org}[UFA]_{org} - k_6'[AA]_{aq}[Ep^*]_{org} \quad (25)$$

$$\frac{d[PAA]_{aq}}{dt} = k_2[IC1]_{aq}[PA]_{aq} - k_4'[PAA]_{org}[UFA]_{org} \quad (26)$$

$$\frac{d[H_2O]_{aq}}{dt} = k_2[IC1]_{aq}[PA]_{aq} - k_7'[H_2O]_{aq}[Ep^*]_{org} \quad (27)$$

$$\frac{d[PA]_{aq}}{dt} = -k_2[IC1]_{aq}[PA]_{aq} \quad (28)$$

$$\frac{d[Ep]_{org}}{dt} = k_4'[PAA]_{org}[UFA]_{org} - k_5'[H^-]_{aq}[Ep]_{org} \quad (29)$$

$$\frac{d[UFA]_{org}}{dt} = -k_4'[PAA]_{org}[UFA]_{org} \quad (30)$$

$$\frac{d[P1]_{org}}{dt} = k_6'[AA]_{aq}[Ep^*]_{org} \quad (31)$$

$$\frac{d[P2]_{org}}{dt} = k_7'[H_2O]_{aq}[Ep^*]_{org} \quad (32)$$

$$[Ep^*]_{org} = \frac{k_5'[H^+]_{aq}[Ep]_{org}}{k_6'[AA]_{aq} + k_7'[H_2O]_{aq}} \quad (33)$$

$$k_4' = \frac{k_4}{K_{PAA}},\ k_5' = \frac{k_5}{K_{H^+}},\ k_6' = \frac{k_6}{K_{AA}},\ and\ k_7' = \frac{k_7}{K_{H_2O}} \quad (34)$$

which are solved by the numerical Runge-Kutta method. The values of the reaction rate constants can be calculated by minimizing the sum of square of errors (SSE) (Equation (35). The experimental data used in determining these constants are derived from previously published data [23].

The initial condition (t = 0):

$$[AA]_{aq} = ([AA]_{aq})_0 \qquad [H^+]_{aq} = ([H^+]_{aq})_0$$

$$[H_2O]_{aq} = ([H_2O]_{aq})_0 \qquad [PAA]_{aq} = 0$$

$$[PA]_{aq} = ([PA]_{aq})_0 \qquad [UFA]_{org} = ([UFA]_{org})_0$$

$$[Ep]_{org} = 0 \qquad [P_1]_{org} = 0 \qquad [P_2]_{org} = 0$$

By determining the values of k_1, k_{-1}, k_2, k_4', k_5', k_6', and k_7' and solving the simultaneous ordinary differential equations (ODE), the concentration of UFA and *Ep* at various time points can be calculated.

$$SSE = \sum \{[UFA]_{calc} - [UFA]_{dt}\}^2 + \sum \{[Ep]_{calc} - [Ep]_{dt}\}^2 \quad (35)$$

3. Results and Discussions

3.1. Effects of Catalyst Concentration

Figures 1, 2, and 3 illustrate the correlation between the iodine values (IV), the conversion to oxirane, and selectivity with reaction time at various catalyst concentrations, respectively. Figure 1 shows that the IV decreased slowly during epoxidation time in the non-catalyst reaction. The addition of catalyst in the reaction provided a considerable effect, resulting in a sharp increase in the conversion of double bonds into epoxidized Tung oil. This was demonstrated by a relatively rapid decline in the IV for various catalyst concentrations (1.5, 3, and 4.5% w/w). It was evident that the IV reduction in the reaction with catalyst was much faster than that of the reaction lacking catalyst. Overall, increasing the catalyst concentra-

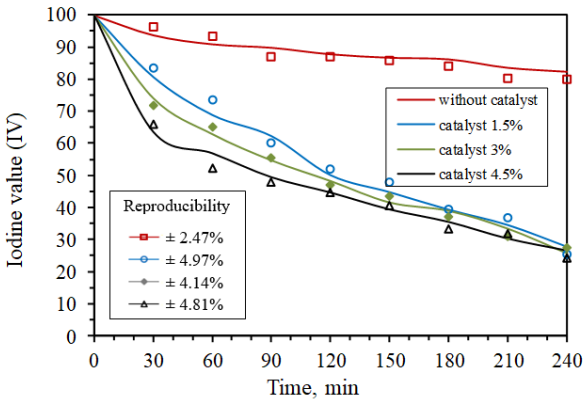

Figure 1. Effects of the catalyst concentration and reaction time on iodine value

tion resulted in a lower IV. This observation was consistent with previously reported results [8].

However, as the reaction reached 120 min, no significant difference was observed for the different amounts of (1.5, 3, and 4.5%) catalyst used. The epoxidation reaction occurred in the organic phase, while sulfuric acid was in aqueous phase. Therefore, as a catalyst, sulfuric acid has to be transferred from the aqueous phase to the organic phase. However, sulfuric acid in the organic phase (oil phase) is very low (limited solubility). It is then irrespective of how high the concentration of sulfuric acid is always in saturated concentration. Hence, at this condition, the rate of epoxidation reaction (in the oil phase) is essentially not affected by sulfuric acid concentration in the aqueous phase, because the sulfuric acid concentration in the oil phase is constant. This phenomenon can be applied to describe that at the reaction time 120 minutes and more, there is no significant different on the resulted IV at 1.5%, 3%, and 4.5% of sulfuric acid catalyst. The final IV value for the catalyzed epoxidation was approximately 30 g I_2/100 g.

Based on the results shown in Figure 2, in the non-catalyst reactions, the conversion to oxirane rose slowly with increasing time without decline. Meanwhile, in the catalytic reactions (for a catalyst concentration of 1.5%, 3%, and 4.5%), longer reaction times produced a considerable increase in the conversion to oxirane until a certain value was reached, followed by a slight decline. This observation indicates that the catalyst significantly affected the reaction rate of the epoxidation of Tung oil, compared to the non-catalytic one. Furthermore, epoxidation with a catalyst concentration of 1.5% resulted in a slightly different oxirane number, when compared to catalyst concentrations of 3% and 4.5%. Considerable difference in conversion to oxirane was only shown in the beginning of reaction time. At a reaction time of 210 min, various catalyst concentrations produced a similar conversion to oxirane (approximately 47%). This was due to the catalyst concentration in the organic or oil phase approached saturation, as mentioned in the previous section of this discussion.

Figure 3 shows that the selectivity in the catalytic epoxidation tended to fluctuate or unstable along the reaction time. On the other hand, the non-catalytic reaction during the reaction time provided consistent selectivity, that was, longer reaction time resulted in the decrease of the reaction selectivity. This was due to the longer reaction time, which promoted the occurrence of side reactions, especially the oxirane ring cleavage reaction. Overall, it can be considered that higher catalyst concentration used in the epoxidation reaction led to lower reaction selectivity. Based on the overall results, the concentration of sulfuric acid catalyst at 1.5% can be considered as the optimum concentration. With reaction times at 210 min and more, a catalyst concentration of 1.5% can produce similar results to that of higher catalyst concentration. These observations are consistent with results obtained in previous studies [8,11] in which the optimum catalyst concentration was 1 to 2%.

3.2. Effects of the Mole Ratio of H_2O_2 to Unsaturated Fatty Acids

H_2O_2 is an oxidizing agent that breaks down double bonds in the epoxidation process. Unfortunately, hydrogen peroxide cannot react with

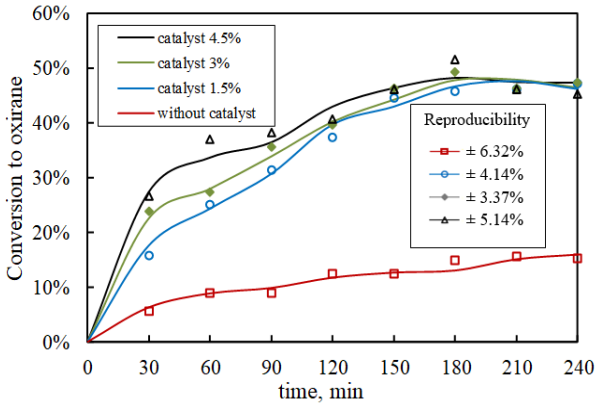

Figure 2. Conversion to oxirane as a function of reaction time at various catalyst concentration

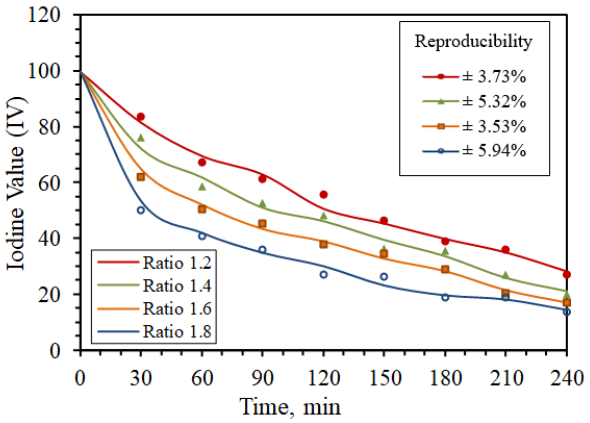

Figure 3. Selectivity as a function of the catalyst concentration and reaction time

the carbon double bond directly to produce an epoxide bond. Therefore, H_2O_2 was reacted first with AA to produce peracetic acid (a strong oxidizer). The mole ratio of H_2O_2 to UFA was evaluated to investigate its effect on the IV, oxirane conversion, and selectivity.

Figure 4 presents IV as a function of the mole ratio of H_2O_2 to UFA and reaction time. The mole ratios of 1.2, 1.4, 1.6, and 1.8 were used. From Figure 4, it can be seen that a higher mole ratio results in a lower IV. This observation suggests that the number of double bonds in UFA moles that reacted with PAA was greater, as a result of an increase in H_2O_2 attack on double bonds. The differences in the IV decrease for various mole ratios were relatively stable with reaction time but became smaller for mole ratios of 1.6 and 1.8 beyond 210 min of reaction time. At the end of the reaction time (240 minutes), the obtained IV for the ratio of 1.8 was 14.2572 g-I_2/100 g.

Figure 5 presents the correlation between the conversion to oxirane and the mole ratio of H_2O_2 to UFA at various reaction times. In all mole ratios, the conversion increased significantly to a maximum value at a certain time and then decreased steadily. The decline occurred at different reaction times for the mole ratios of 1.2, 1.4, 1.6, and 1.8, corresponding to 240, 210, 210, and 180 minutes, respectively. A higher mole ratio accelerated the process to reach its maximum potential. This observation was appropriate with previously published results [8,30]. At a mole ratio of H_2O_2 to UFA beyond 1.6 and a reaction time of 150 minutes or longer, the conversion decreased, because side reactions became more dominant with increasing reaction time. At a reaction time of 210 minutes, the mole ratio of 1.2, 1.4, and 1.6 resulted in a similar conversion value, which was approximately 47%. The highest observed conversion value was 48.94% for a mole ratio of 1.6.

Figure 6 demonstrates selectivity as a function of the mole ratio of H_2O_2 to UFA and reaction time. Selectivity is the amount of the UFA mole that is converted to oxirane divided by the total reacted mole of UFA. Figure 6 demonstrates that selectivity fluctuated slightly during the reaction time and was directly proportional to the mole ratio. An increasing mole ratio enhanced the selectivity value. Taking into consideration the IV, oxirane conversion, and selectivity, the mole ratio of 1.6 was recommended as the optimum ratio in this study. This recommendation was focused on achieving an optimal conversion. The resulted optimum mole ratio was different than those reported in previous studies, such as 2.0 and 1.5 [11,30], because of differences in vegetable oil characteristics.

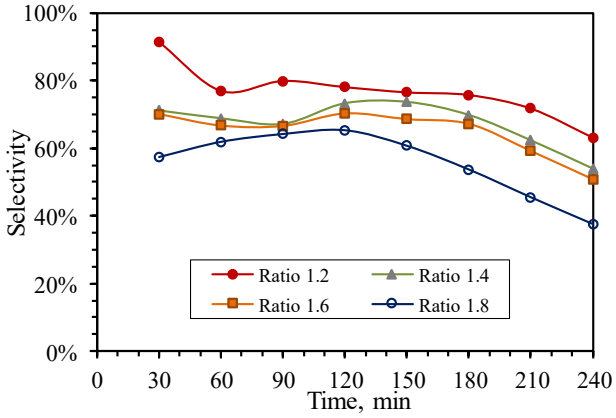

Figure 6. Selectivity as a function of the mole ratio of H_2O_2 to UFA and reaction time

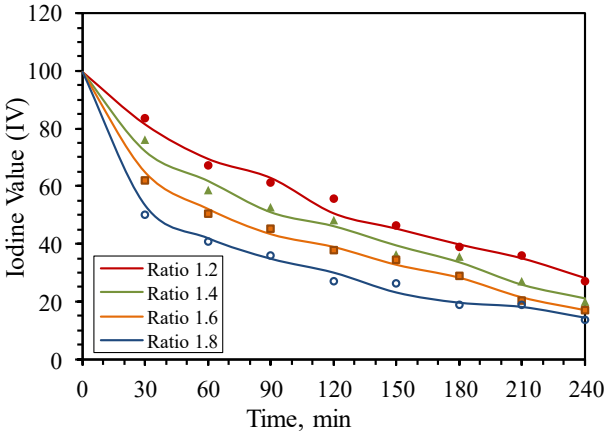

Figure 4. Effects of the mole ratio of H_2O_2 to UFA and reaction time on iodine value

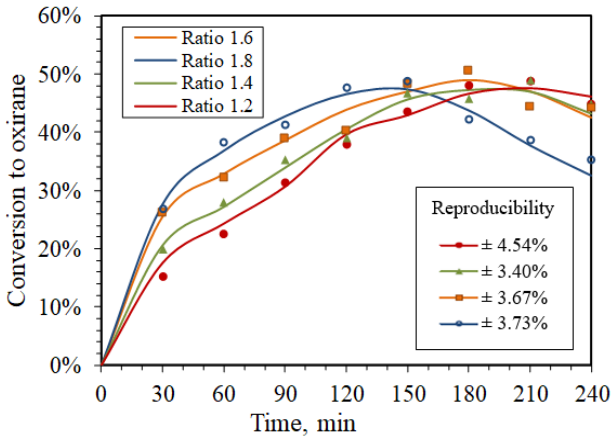

Figure 5. Conversion to oxirane as a function of the mole ratio of H_2O_2 to UFA and reaction time

3.3. Evaluation of the Kinetics Model

Figure 7 shows the program results, which demonstrate the comparison between experimental and modeling data for differing concentrations of UFA and epoxidized Tung oil (EP) at temperatures of 40, 50, 60, and 70°C. Some constants (k_1, k_{-1}, and k_2) represent reaction rate constants, while k_4', k_5', k_6', and k_7' are a combination of reaction rate and mass transfer constants. The resultant constants with varying orders are shown in Table 1. This observation suggests that there exist both dominant constants and less influential ones. The k_1, k_{-1}, and k_4' constants were the dominant constants

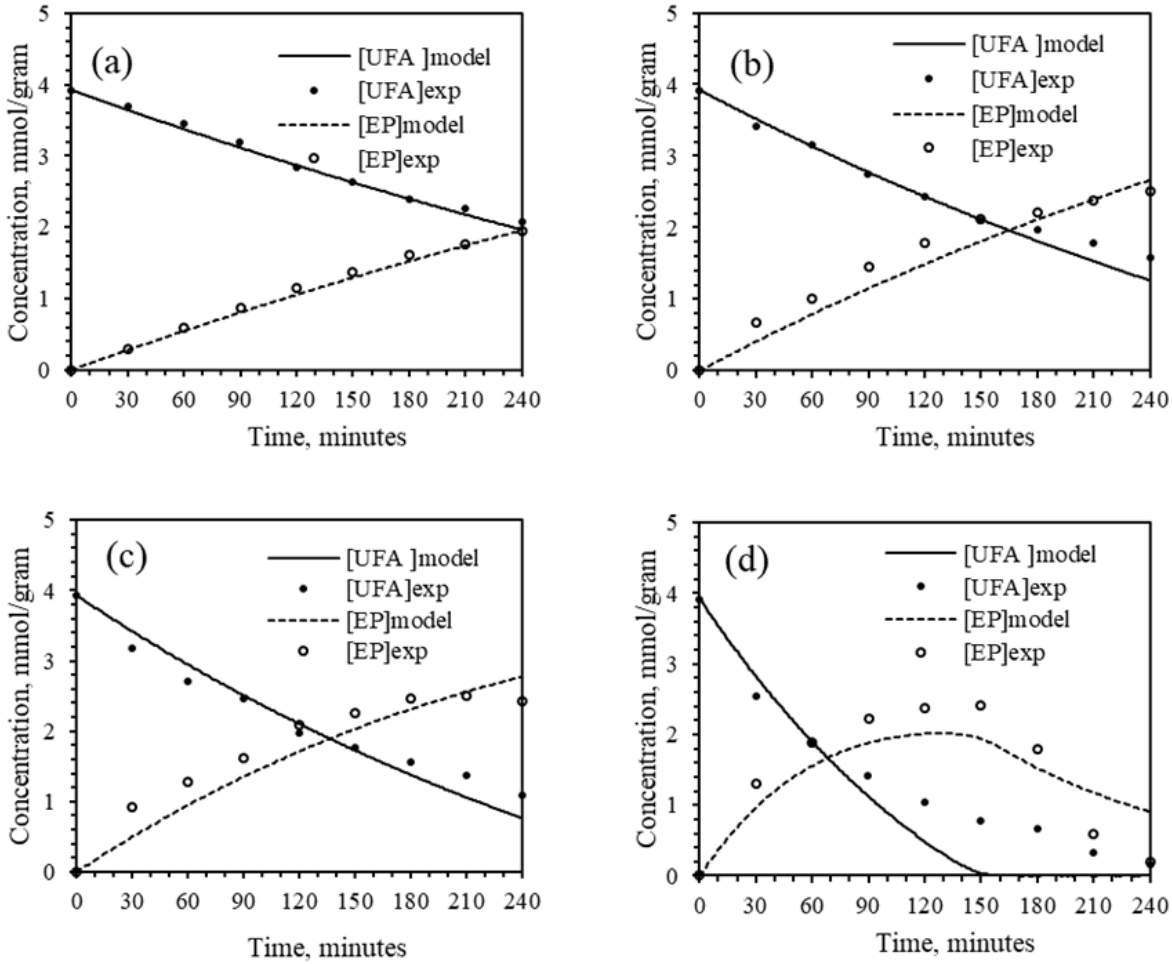

Figure 7. The experimental and model concentrations of UFA and EP as a function of reaction time at various temperatures: (a) 40 °C, (b) 50 °C, (c) 60 °C, and (d) 70 °C

Table 1. Constants for the proposed model

Rate constant	Temperature			
	40 °C	50 °C	60 °C	70 °C
k_1 (g/mol.min)	267.760 ± 0.586*	605.726 ± 0.176	1017.995 ± 1.662	1474.167 ± 0.541
k_{-1}(1/min)	10.572 ± 0.060	29.159 ± 0.022	101.348 ± 0.757	101.348 ± 1.453
k_2 (g/mol.min)	151.640 ± 0.546	262.191 ± 0.107	674.798 ± 0.596	1150.166 ± 0.860
k_4'(g/mol.min)	788.107 ±0.893	1198.095 ± 1.538	1421.954 ± 0.983	1831.988 ± 1.485
k_5'(g/mol.min)	0.004 ± 0.0001	0.005 ± 0.002	7.016 ± 0.286	60.518 ± 0.779
k_6'(g/mol.min)	5.276 ± 0.183	52.307 ± 0.290	464.010 ± 0.343	877.262 ± 0.663
k_7'(g/mol.min)	5.266 ± 0.173	52.581 ± 0.156	464.326 ± 0.436	878.196 ± 0.930

*mean ± deviation

at all reaction temperatures, while the values of k_5', k_6', and k_7' were relatively small, especially at low temperatures. However, the last three constants were very sensitive to temperature increases when compared to the others. For example, the values of k_5' at temperatures of 40 and 70 °C were 0.004 and 60.518 g/mol. min, respectively (14,000-fold with a temperature increase of 30 °C). Another important point was that the evaluated kinetics model provided satisfactory results, whereas the experimental data of UFA and EP concentrations were close to that proposed by the model. Even for a temperature of 40 °C, the results from the model fit perfectly with the experimental data (SSE less than 5%). At higher temperatures, relative or SSE errors were greater because of the possible occurrence of other adverse reactions.

One of the representative and commonly used equations for determining the parameters of kinetic constants is the Arrhenius equation. The activation energy (E_a) and collision factor (A) were evaluated by linearization of ln k_i versus $1/T$ for each constant. Table 2 demonstrates a good fit linearization of the Arrhenius equations acquired for all the constant reaction rates, shown by the high values of R^2. The lowest R^2 value was relatively high and was obtained for k_5', which represented the kinetics constant in the protonation of epoxidized Tung oil.

The values of A, E_a, and mean R^2 are shown in Table 2. The obtained activation energy (E_a) values were not considerably different for all constants, except k_4' (the value was relatively low when compared to others). These values (E_a of k_1, k_{-1}, and k_2) were consistent with previously reported results, such as: the epoxidation of MEPOL, which generated 15.1 kcal/mol [28] and rubber seed oil, which gained 15.7 kcal/mol [4]. Moreover, 11.7 kcal/mol was reported for cottonseed oil [9], 14.9, and 14.5 kcal/mol were reported in previous studies [7,6] for karanja oil and mahua oil, respectively.

4. Conclusions

Sulfuric acid, as a catalyst in the epoxidation of Tung oil, played an important role and showed benefits, which gave noticeable and better conversion to oxirane, compared to reactions conducted without catalysts. A higher catalyst concentration decreased selectivity and produced a fluctuating value of selectivity for the reaction times used. Overall, an increase in mole ratio resulted in a lower IV, a higher conversion to oxirane, and a decrease in selectivity. The mole ratio of 1.6 and catalyst concentration of 1.5% were recommended to be the optimum values obtained in this study. The proposed kinetics model provided good results and was suitable for all variations in reaction temperature. Even at a temperature of 40 °C, an excellent fit was obtained between the experimental data and the model data.

Acknowledgement

The authors gratefully acknowledge financial support to "*Deputi Bidang Penguatan Riset dan Pengembangan, Kementerian Riset dan Teknologi / Badan Riset dan Inovasi Nasional, Republik Indonesia*" for research funding through "*Hibah Penelitian Disertasi Doktor*" with agreement number 2095/UN1/DITLIT/DIT-LIT/PT/2020.

Table 2. The resultant E_a, A, and mean R^2 values

Constants	A (g/mol.min)*	E_a (kcal/mol)	Mean R^2 value
k_1	$(8.057 \pm 0.145) \times 10^{10}$	12.0415 ± 0.0121	0.9776
k_{-1}	$(2.436 \pm 0.842) \times 10^{13}$	17.5631 ± 0.2682	0.9167
K2	$(4.149 \pm 0.176) \times 10^{12}$	14.9341 ± 0.0278	0.9864
k_4'	$(9.061 \pm 0.224) \times 10^{6}$	5.7663 ± 0.0164	0.9737
k_5'	$(3.271 \pm 0.204) \times 10^{50}$	76.2442 ± 0.6280	0.8884
k_6'	$(1.236 \pm 0.474) \times 10^{27}$	37.4704 ± 0.117	0.9607
k_7'	$(1.255 \pm 0.465) \times 10^{27}$	37.4795 ± 0.2061	0.9606

*the unit of A for k_{-1} is 1/min

Nomenclature

A : collision factor (g/mol.min, except for k_{-1} (1/min))
AA : acetic acid
$[AA]_{aq}$: acetic acid concentration in aqueous phase (mol/g)
$[AA]_{org}$: acetic acid concentration in organic phase (mol/g)
E_a : activation energy (kcal/mol)
E_p : epoxidized Tung oil
$[E_p]_{org}$: epoxidized Tung oil concentration in organic phase (mol/g)
E_p^* : protonated epoxidized Tung oil
$[E_p^*]_{org}$: protonated epoxidized Tung oil concentration in organic phase (mol/g)
H^+ : acid catalyst
$[H^+]_{aq}$: catalyst concentration in aqueous phase (mol/g)
$[H^+]_{org}$: catalyst concentration in organic phase (mol/g)
H_2O : water
IC_1 : intermediate compound 1
$[IC_1]_{aq}$: intermediate compound 1 concentration in aqueous phase (mol/g)
IV : iodine value (g-I_2/100 g sample)
IV_0 : initial iodine value (g-I_2/100 g sample)
k_1 : kinetic rate constant for forward reaction, Eq. (7) (g/mol.min)
k_{-1} : kinetic rate constant for backward reaction, Eq. (7) (1/min)
k_2 : kinetic rate constant, Eq. (8) (g/mol.min)
K_{AA} : equilibrium constant for AA, Eq. (16)
K_{H+} : equilibrium constant for H^+, Eq. (17)
K_{H2O} : equilibrium constant for H_2O, Eq. (18)
K_{PAA} : equilibrium constant for PAA, Eq. (19)
k_4', k_5' : ratio of reaction rate constant to equilibrium constant of AA, and H^+ (g/mol.min)
k_6', k_7' : ratio of reaction rate constant to equilibrium constant of H_2O, and PAA (g/mol.min)
P1 : side product 1
$[P1]_{org}$: side product 1 concentration in organic phase (mol/g)
P2 : side product 2
$[P2]_{org}$: side product 2 concentration in organic phase (mol/g)
PA : hydrogen peroxide
$[PA]_{aq}$: hydrogen peroxide concentration in aqueous phase (mol/g)
$[PA]_{org}$: hydrogen peroxide concentration in organic phase (mol/g)
PAA : peroxyacetic acid
$[PAA]_{aq}$: peroxyacetic acid concentration in aqueous phase (mol/g)
$[PAA]_{org}$: peroxyacetic acid concentration in organic phase (mol/g)
R : universal gas constant (kcal/mol.K)
t : reaction time (minute)
T : temperature (K)
UFA : unsaturated fatty acids
$[UFA]_{org}$: unsaturated fatty acids concentration in organic phase (mol/g)

References

[1] Carbonell-Verdu, A., Samper, M.D., Garcia-Garcia, D., Sanchez-Nacher, L., and Balart, R. (2017). Plasticization effect of epoxidized cottonseed oil (ECSO) on poly(lactic acid). *Industrial Crops and Products*, 104, 278–286. DOI: 10.1016/j.indcrop.2017.04.050.

[2] Brodin, M., Vallejos, M., Opedal, M.T., Area, M.C., and Chinga-Carrasco, G. (2017). Lignocellulosics as sustainable resources for production of bioplastics – a review. *Journal of Cleaner Production*, 162, 646–664. DOI: 10.1016/j.jclepro.2017.05.209.

[3] Cooney, T.I., Cardona, F., and Tran-Cong, T. (2011). Kinetics of in-situ epoxidation of hemp oil under heterogeneous reaction conditions: an overview with preliminary results. In: *EddBE2011: 1st International Postgraduate Conference on Engineering*, Designing and Developing the Built Environment for Sustainable Wellbeing, Queensland University of Technology, 106–111.

[4] Okieimen, F., Bakare, O., and Okieimen, C. (2002). Studies on the epoxidation of rubber seed oil. *Industrial Crops and Products*, 15, 139–144. DOI: 10.1016/S0926-6690(01)00104-2.

[5] Kamalakar K., Rajak A.K., Prasad R.B.N., and Karuna M.S.L. (2013). Rubber seed oil based biolubricant basestocks: A potential source for hydraulic oils. *Industrial Crops and Products*, 51, 249-257. DOI: 10.1016/j.indcrop.2013.08.058.

[6] Park, S.-J., Jin, F.-L., and Lee, J.-R. (2004). Effect of biodegradable epoxidized castor oil on physicochemical and mechanical properties of epoxy resins. *Macromolecular Chemistry and Physics*, 205, 2048–2054. DOI: 10.1002/macp.200400214.

[7] Borugadda V.B., and Goud V.V. (2014). Epoxidation of castor oil fatty acid methyl esters (COFAME) as a lubricant base stock using heterogeneous ion-exchange resin (IR-120) as a catalyst. *Energy Procedia,* 54, 75 – 84. DOI: 10.1016/j.egypro.2014.07.249.

[8] Goud, V.V., Patwardhan, A.V., and Pradhan, N.C. (2006). Studies on the epoxidation of

mahua oil (Madhumica indica) by hydrogen peroxide. *Bioresource Technology*, 97, 1365–1371.

[9] Goud, V.V., Pradhan, N.C., and Patwardhan, A.V. (2006). Epoxidation of karanja (Pongamia glabra) oil by H_2O_2. *Journal of the American Oil Chemists' Society*, 83, 635–640. DOI: 10.1016/j.biortech.2005.07.004.

[10] Goud, V.V., Patwardhan, A.V., and Pradhan, N.C. (2007). Kinetics of in-situ epoxidation of natural unsaturated triglycerides catalyzed by acidic ion exchange resin. *Industrial and Engineering Chemistry Research*, 46, 3078–3085. DOI: 10.1021/ie060146s.

[11] Dinda, S., Patwardhan, A.V., Goud, V.V., and Pradhan, N.C. (2008). Epoxidation of cottonseed oil by aqueous hydrogen peroxide catalysed by liquid inorganic acids. *Bioresource Technology*, 99, 3737–3744. DOI: 10.1016/j.biortech.2007.07.015.

[12] Dinda, S., Ravisankar, V., and Puri, P. (2016). Development of Bio-epoxide from Nahor (Mesua ferrea Linn) Oil. *Journal of the Taiwan Institute of Chemical Engineers*, 65, 399–404. DOI: 10.1016/j.jtice.2016.05.053.

[13] Omonov, T.S., Kharraz, E., and Curtis, J.M. (2016). The epoxidation of canola oil and its derivatives. *RSC Advances*, 6, 92874–92886. DOI: 10.1039/C6RA17732H.

[14] Omonov T.S., Kharraz E., and Curtis J.M. (2017). Camelina (Camelina Sativa) oil polyols as an alternative to Castor oil. *Industrial Crops and Products*, 107, 378-385. DOI: 10.1016/j.indcrop.2017.05.041.

[15] Baumstark A.L., Franklin P.J., Vasquez P.C., and Crow B.S. (2004). Kinetics of the epoxidation of geraniol and model systems dimethyldioxirane. *Molecules*, 9, 117–24. DOI: 10.3390/90300117.

[16] Kousaalya, A.B., Beyene, S.D., Gopala, V., Ayalew, B., and Pilla, S. (2018). Green epoxy synthesized from Perilla frutescens: A study on epoxidation and oxirane cleavage kinetics of high-linolenic oil. *Industrial Crops and Products*, 123, 25–34. DOI: 10.1016/j.indcrop.2018.06.047.

[17] Vossen, H.A.M., and Umali, B.E. (2002). Plant Resources of South-East Asia No 14. *Prosea Foundation*, Bogor, Indonesia, 113–115.

[18] Panchal, B., Chang, T., Qin, S., Sun, Y., Wang, J., and Bian. K. (2020). Optimization and kinetics of Tung nut oil transesterification with methanol using novel solid acidic ionic liquid polymer as catalyst for methyl ester synthesis. *Renewable Energy*, 151, 796-804. DOI: 10.1016/j.renene.2019.11.066.

[19] Feng, Y., Man, L., Hu, Y., Chen, L., Xie, B., Zhang, C., Yuan, T., and Yang. Z. (2019). One-pot synthesis of polyurethane-imides with tailored performance from castor and Tung oil. *Progress in Organic Coatings*, 132, 62–69. DOI: 10.1016/j.porgcoat.2019.03.035.

[20] Gallart-Sirvent, P., Li, A., Li, K., Villorbina, G., and Canela-Garayoa, R. (2017). Preparation of pressure-sensitive adhesives from Tung oil via Diels-Alder reaction. *International Journal of Adhesion and Adhesives*, 78, 67-73. DOI: 10.1016/j.ijadhadh.2017.06.021.

[21] Liang, B., Kuang, S., Huang, J., Man, L., Yang, Z., and Yuan, T. (2019). Synthesis and characterization of novel renewable Tung oil-based UVcurable active monomers and bio-based copolymers. *Progress in Organic Coatings*, 129, 116–124. DOI: 10.1016/j.porgcoat.2019.01.007.

[22] Li, M., Li, S., Xia, J., Ding, C., Wang, M., Xu, L., Yang, X., and Huang, K. (2017). Tung oil based plasticizer and auxiliary stabilizer for poly(vinyl chloride). *Materials and Design*, 122, 366–375. DOI: 10.1016/j.matdes.2017.03.025.

[23] Budiyati, E., Budhijanto, Budiman, A., and Rochmadi. (2020). Kinetic study of epoxidation of Tung oil (Reutealis trisperma (Blanco) Airy Shaw) by peroxyacetic acid. *IOP Conference Series: Materials Science and Engineering*, vol 778: 012002. DOI: 10.1088/1757-899X/778/1/012048.

[24] Zaher, F.A., El-Mallah, M.H., and El-Hefnawy, M.M. (1989). Kinetics of oxirane cleavage in epoxidized soybean oil. *Journal of American Oil Chemists' Society*, 66, 698–700. DOI: 10.1007/BF02669955.

[25] Rangarajan, B., Havey, A., Grulke, E.A., and Culnan, P.D. (1995). Kinetic parameters of a two-phase model for in-situ epoxidation of soybean oil. *Journal of American Oil Chemists' Society*, 72, 1161–1169. DOI: 10.1007/BF02540983.

[26] Petrovic, A.S., Zlatanic, A., Lava, C.C., and Sinadinovic-Fiser, S. (2002). Epoxidation of soybean oil in toluene with peroxoacetic acid and peroxoformic acids-kinetics and side reactions. *European Journal of Lipid Science and Technology*, 104, 293–299. DOI: 10.1002/1438-9312(200205)104:5<293::AID-EJLT293>3.0.CO;2-W.

[27] Cai, C., Dai, H., Chen, R., Su, C., Xu, X., Zhang, S., and Yang, L. (2008). Studies on the kinetics of in-situ epoxidation of vegetable oils. *European Journal of Lipid Science and Technology*, 110, 341–346. DOI: 10.1002/ejlt.200700104.

[28] Wu, Z., Nie, Y., Chen, W., Wu, L., Chen, P., Lu, M., Yu, F., and Ji, J. (2016). Mass transfer and reaction kinetics of soybean oil epoxidation in a formic acid-autocatalyzed reaction system. *Canadian Journal of Chemical Engineering*, 94, 1576–1582. DOI: 10.1002/cjce.22526.

[29] Sienkiewicz, A.M., and Czub, P. (2016). The unique activity of catalyst in the epoxidation of soybean oil and following reaction of epoxidized product with bisphenol A. *Industrial Crops and Products*, 83, 755–773. DOI: 10.1016/j.indcrop.2015.11.071.

[30] Mungroo, R., Pradhan, N.C., Goud, V.V., and Dalai, A.K. (2008). Epoxidation of canola oil with hydrogen peroxide catalyzed by acidic ion exchange resin. *Journal of American Oil Chemists' Society*, 85, 887–896. DOI:10.1007/s11746-008-1277-z.

[31] Monono, E.M., Haagenson, D.M., and Wiesenborn, D.P. (2015). Characterizing the epoxidation process conditions of canola oil for reactor scale-up. *Industrial Crops and Products*, 67, 364–372. DOI: 10.1016/j.indcrop.2015.01.061.

[32] de Haro, J.C., Izarra, I., Rodríguez, J.F., Perez, A., and Carmona, M. (2016). Modelling the epoxidation reaction of grape seed oil by peracetic acid. *Journal of Cleaner Production*, 138, 70-76. DOI: 10.1016/j.jclepro.2016.05.015.

[33] Goud, V.V., Patwardhan, A.V., Dinda, S., and Pradhan, N.C. (2007). Kinetics of epoxidation of jatropha oil with peroxyacetic and peroxyformic acid catalysed by acidic ion exchange resin. *Chemical Engineering Science*, 62, 4065–4076. DOI: 10.1016/j.ces.2007.04.038.

[34] Gan, L.H., Goh, S.H., and Ooi, K.S. (1992). Kinetic studies of epoxidation and oxirane cleavage of palm olein methyl esters. *Journal of American Oil Chemists' Society*, 69, 347–351. DOI: 10.1007/BF02636065.

[35] Janković, M.R., Sinadinović-Fišer, S.V., and Govedarica, O.M. (2014). Kinetics of the epoxidation of castor oil with peracetic acid formed in-situ in the presence of an ion exchange resin. *Industrial Engineering and Chemistry Research*, 53, 9357–9364. DOI: 10.1016/j.cep.2012.08.005.

[36] Ikhuoria E.U., Obuleke R.O., Okieimen F.E. (2007). Studies on the kinetics of epoxidation of the methyl esters of parkia biglobosa seed oil. *Journal of Macromolecular Science, Part A: Pure and Applied Chemistry*, 44, 235–238. DOI: 10.1080/10601320601031424.

[37] Paquot, C. (1979). Standard Methods for the Analysis of Oils, Fats, and Derivatives, Part 1. *sixth ed. Pergamon*, Oxford, 66–70.